J. Webster (ed.), *Wiley Encyclopedia of Electrical and Electronics Engineering*

PREAMPLIFIERS

The essential task of sensors, detectors, and transducers is to convert the characteristics of the physical world (e.g., light, sound, pressure, displacement, temperature) into electrical signals, which are then suitably processed for the required application. Before being processed, these electrical signals must be conditioned by appropriate electronic circuitry.

Despite the improvements carried out in recent years, all sensors have a common characteristic: a weak signal delivered and a limiting noise level. Therefore, the front end of the sensor-associated electronic system must be an amplifier, usually called a *preamplifier.* Two main requirements must be satisfied for preamplifiers. First, they must raise the signal level adequately over a certain frequency range (linear amplification is very often requested). Second, they must contribute only a minimum amount of additional noise. Depending on the specific application, other features such as high linearity, large output swing, wide-band operation, and large output drive capability may be needed, but these requirements do not differ substantially from those of normal amplifiers. What is specifically important for preamplifiers is to optimize their noise performance. This is because, although the noise performance of a generic electronic system [which is made up of a preamplifier, signal conditioning and processing circuitry, and output interface (Fig. 1)] depends on the noise behavior of all these subsystems, in practice, in a well-designed system the noise performance is entirely dominated by the noise characteristics of the front-end circuit (preamplifier). This is true if the preamplifier gain is sufficiently high to allow the subsequent processing to be performed with negligible degradation in the signal-to-noise ratio. Hence, low-noise system design is mainly focused on low-noise preamplifier design.

Basic Concepts Related with Preamplifiers

Some basic concepts useful in analyzing preamplifiers from the noise standpoint, namely, equivalent input noise, noise factor and noise figure, and noise matching, are introduced in this section.

Equivalent Input Noise. In the characterization of many nonideal electrical quantities, which are generated by a plurality of sources or mechanisms within a circuit, it is a common practice to replace all by one equivalent input source. This equivalent source has the same effect at the circuit output as the global effect of all the individual internal sources and, therefore, the circuit can be considered free of such mechanisms (1), which greatly simplifies circuit analysis and design. Offset voltage and noise are representative examples of what has been discussed.

A network, such as an amplifier, is made up of many components. Any electrical component has its own internal mechanisms of noise generation. As a result, the output of any real amplifier exhibits noise, which depends on factors such as internal noise sources, circuit topology, gain, and measurement bandwidth. The amplifier's output noise power spectral density can be found by multiplying the noise power spectral density of each source by the squared module of its particular transfer function and then superposing all the individual noise contributions. This procedure must be followed for any frequency of interest.

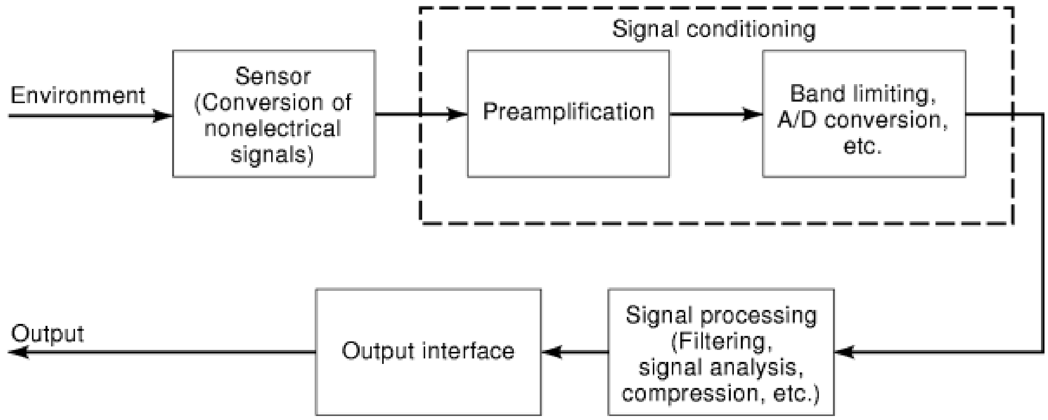

Fig. 1. The electronic chain associated with a sensor includes a preamplifier, signal conditioning and processing circuitry, and output interface. The stages cascaded to the preamplifier may provide additional gain.

Rather than by the noise measured at its output, an amplifier is best characterized by the minimum signal applied to its input, which is still detectable at the output of the signal processor. This signal may be conveniently regarded as equivalent to a virtual noise source located at the input. This is known as *equivalent input noise* or *input-referred noise* of the amplifier, and allows one to easily compare the total noise generated by the amplifier with the input signal. From the above considerations, the equivalent input noise power of an amplifier coincides with the output noise power divided by the squared module of the amplifier gain (2).

A similar idea is applied to the noise model of a generic sensor. Starting from its small-signal equivalent circuit, including all impedances and current/voltage signal generators, a noise equivalent circuit is derived by including the noise sources associated with resistances (or, better, with the real parts of impedances) and signal generators. From this equivalent noise circuit, an expression for small-signal gain and equivalent input noise is derived.

Figure 2(a) represents the equivalent noise circuit of a generic system consisting of a sensor and a preamplifier. The sensor is described by its signal voltage generator V_{s}, its internal series impedance Z_{s}, and a noise voltage generator, $V_{\mathrm{n,s}}$, which includes the contributions by all sensor noise sources. The preamplifier, having voltage gain A_{v} and input impedance Z_{i}, is represented from the noise point of view, by a noise voltage generator $V_{\mathrm{n,a}}$ and a noise current generator $I_{\mathrm{n,a}}$ placed in series and in parallel, respectively, with the input port. These noise generators, whose magnitude is specified in units of V/(Hz)$^{1/2}$ and A/(Hz)$^{1/2}$, respectively, are in general, frequency dependent, and are very often represented in terms of their mean square voltage, $V^2{}_{\mathrm{n,a}}$ (V^2/Hz), and mean square current, $I^2{}_{\mathrm{n,a}}$ (A^2/Hz). The two generators can be statistically correlated or not, depending on the specific case. For example, they are practically 100% correlated and totally uncorrelated, respectively, when modeling a metal-oxide-semiconductor (*MOS*) field-effect transistor or a bipolar junction transistor (*BJT*) in the mid-frequency range (3). When combining the effects of different noise sources, one must remember that noise is a random signal. Therefore, when summing two noise variables A_{n} and B_{n}, the result is $C^2{}_{\mathrm{n}} = A^2{}_{\mathrm{n}} + B^2{}_{\mathrm{n}} + 2\,\mathrm{Re}\{A^*{}_{\mathrm{n}}B_{\mathrm{n}}\}$, where $\mathrm{Re}\{A^*{}_{\mathrm{n}}B_{\mathrm{n}}\}$ represents the real part of the cross-correlation spectrum of A_n and B_{n}. For ease of use, the correlation effect between two variables is very often expressed by using the so-called correlation coefficient γ, which is a normalized factor having a value between 0 (no correlation) and 1 (100% correlation). Using this approach, one has $C^2{}_{\mathrm{n}} = A^2{}_{\mathrm{n}} + B^2{}_{\mathrm{n}} + 2\gamma A_{\mathrm{n}}B_{\mathrm{n}}$.

Although the number of noise sources in Fig. 2(a) has been reduced to three, further simplifications are usually carried out to represent them just by one equivalent input noise voltage generator, $V_{\mathrm{n,eq}}$, at the signal source location (2). To derive an expression for the equivalent input noise, the total noise at the amplifier

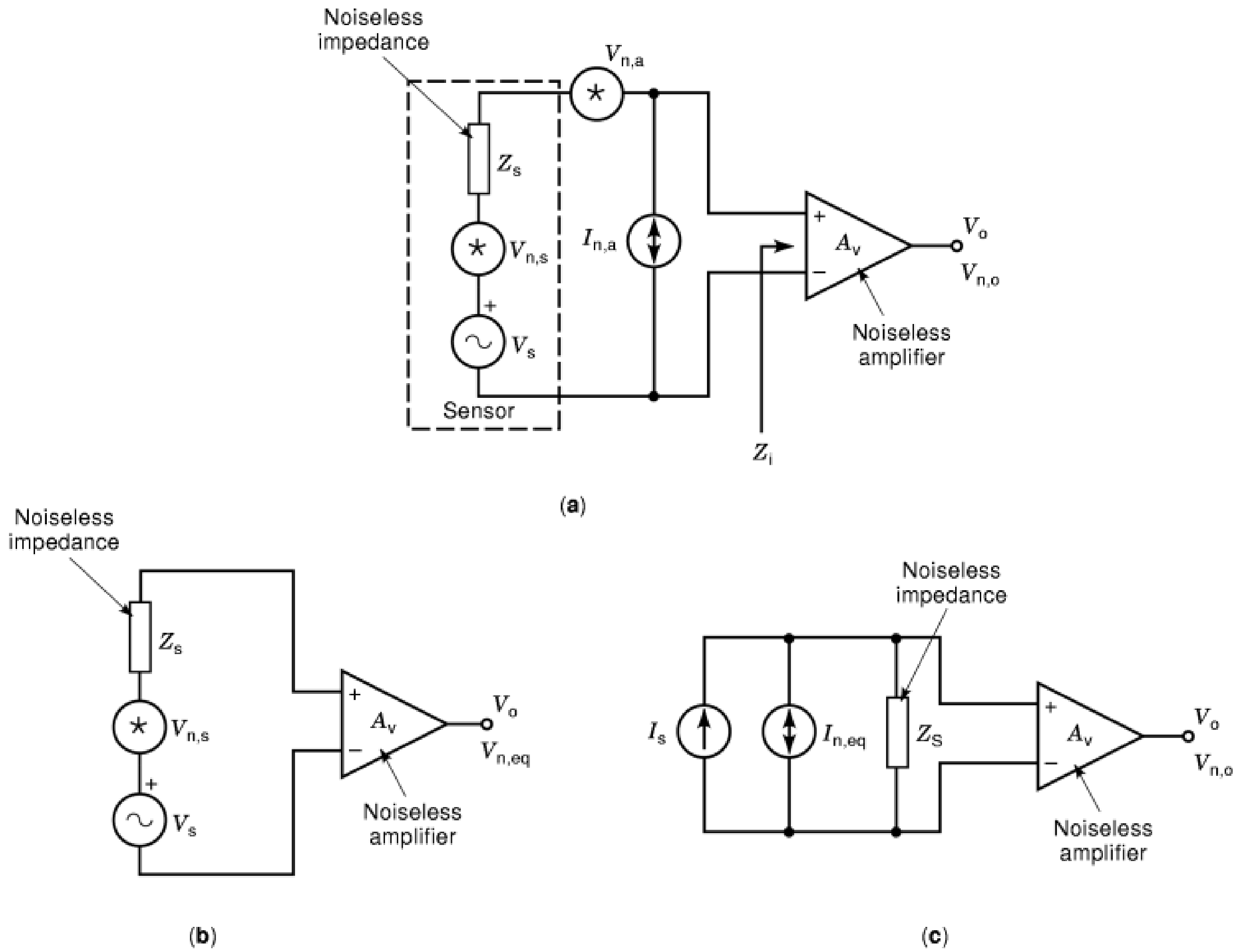

Fig. 2. A generic system noise model (a) can be reduced to an equivalent circuit with an equivalent input noise voltage generator (b), or to an equivalent circuit with an equivalent input noise current generator (c).

output, $V_{n,o}$, must be first derived. Assuming $V_{n,a}$ and $I_{n,a}$ to be statistically uncorrelated, one obtains:

$$V_{n,o}^2 = (V_{n,a}^2 + V_{n,s}^2) \cdot |A_v|^2 \cdot \left|\frac{Z_i}{Z_i + Z_s}\right|^2 + I_{n,a}^2 \cdot |A_v|^2 \cdot \left|\frac{Z_i \cdot Z_s}{Z_i + Z_s}\right|^2 \tag{1}$$

The system gain from the signal source location is

$$A_v' = A_v \frac{Z_i}{Z_i + Z_s} \tag{2}$$

Therefore, the equivalent input noise voltage, $V_{n,eq}$, which is equal to the total output noise divided by the squared module of the system gain, is given by;

$$V^2_{n,eq} = \frac{V^2_{n,o}}{|A'_v|^2} = V^2_{n,a} + V^2_{n,s} + I^2_{n,a} \cdot |Z_s|^2 \qquad (3)$$

After combining and reflecting all noise sources to the signal source location, the resulting equivalent circuit is shown in Fig. 2(b). The noise source $V_{n,eq}$ will generate exactly the output noise given by Eq. (1).

$V^2{}_{n,eq}$ can also be obtained from Fig. 2(a) by disconnecting the noiseless amplifier and evaluating the voltage across the noise generator $I_{n,a}$, which results in Eq. (3). This operation corresponds to finding the equivalent dipole connected at the input of the noiseless amplifier (Thévenin theorem). In practice, the dipole in Fig. 2(a) constituted by V_s, $V_{n,s}$, Z_s, $V_{n,a}$, and $I_{n,a}$, is exactly equivalent to the dipole in Fig. 2(b) constituted by V_s, $V_{n,eq}$, and Z_s.

Observe that, as indicated in Eq. (3), the equivalent input voltage noise does not depend on the amplifier gain and input impedance, although the effect of any noise generated at Z_i is implicit in $I_{n,a}$. However, $V_{n,eq}$ depends on the impedance of the signal source, as well as on the noise generated by the sensor (hence, the design approach for noise optimization will also depend on the kind of sensor impedance, that is resistive, capacitive, inductive, as will be shown below). Output noise will obviously depend on both the gain and the input impedance of the amplifier.

Following similar steps, an equivalent noise circuit of the system can also be derived in terms of an equivalent input noise current generator $I_{n,eq}$ [Fig. 2(c)]:

$$I^2_{n,eq} = I^2_{n,a} + I^2_{n,s} + \frac{V^2_{n,a}}{|Z_s|^2} \qquad (4)$$

where $I^2{}_{n,s} = V^2{}_{n,s}/|Z_s|^2$.

Either equivalent noise circuit can be used, however, it is generally more appropriate to characterize the system noise in the same terms as the source signal (voltage or current).

If the amplifier noise voltage and current generators $V_{n,a}$ and $I_{n,a}$ are not statistically independent, as occurs when they contain some components arising from a common phenomenon, the scheme of Fig. 2(b) must include another noise voltage generator in series with $V_{n,eq}$. The power spectral density of this generator is a function of their correlation coefficient: $V^2{}_n = 2\gamma|V_{n,a}I_{n,a}Z_s|$. In the same way, an additional noise current generator $I^2{}_n = 2\gamma|V_{n,a}I_{n,a}/Z_s|$ has to be placed in parallel with $I_{n,eq}$ in the scheme of Fig. 2(c).

Equivalent Input Noise in Cascaded Stages. Consider the network in Fig. 3, which consists of n cascaded stages having respective voltage gains A_{v1}, A_{v2}, …, A_{vn} and equivalent input noise voltage sources $V_{n,eq1}$, $V_{n,eq2}$, …, $V_{n,eqn}$. It should be pointed out that a "stage" in this figure can be a complex circuit or even a single active device. Moreover, for each stage i ($i = 1, 2, \ldots, n$), A_{vi} and $V_{n,eqi}$ are evaluated taking the value of input and output impedances into account. Assuming that noise sources of different stages are uncorrelated, as is the usual case, the total output noise power is

$$\begin{aligned} V^2_{n,o} = {} & V^2_{n,eq1} \cdot |A_{v1}|^2 \cdot |A_{v2}|^2 \cdots |A_{vn}|^2 + V^2_{n,eq2} \cdot |A_{v2}|^2 \cdots |A_{vn}|^2 \\ & + \cdots + V^2_{n,eqn} \cdot |A_{vn}|^2 \end{aligned} \qquad (5)$$

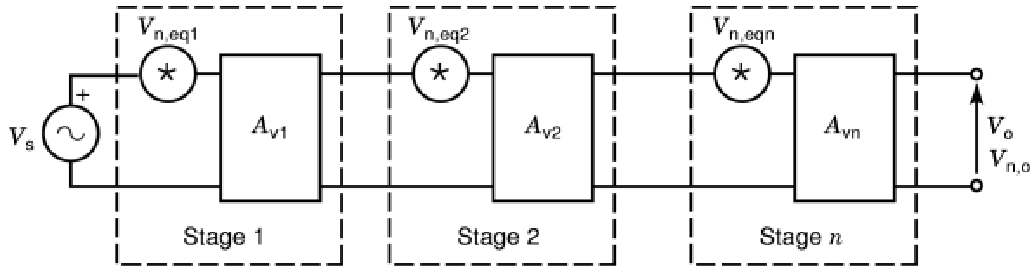

Fig. 3. Schematics for evaluating the noise performance of an n-stage voltage amplifier.

which corresponds to an equivalent input noise for the whole network equal to

$$\begin{aligned} V_{n,eq}^2 &= \frac{V_{n,o}^2}{|A_{v1}|^2 \cdot |A_{v2}|^2 \cdots |A_{vn}|^2} \\ &= V_{n,eq1}^2 + \frac{V_{n,eq2}^2}{|A_{v1}|^2} + \cdots + \frac{V_{n,eqn}^2}{|A_{v1}|^2 \cdot |A_{v2}|^2 \cdots |A_{vn-1}|^2} \end{aligned} \quad (6)$$

From this equation, one concludes that the noise behavior of the whole network can be dominated by the first stage, provided that its voltage gain is large enough. In this case, in fact, noise contributions by the following stages can be neglected. The same conclusion also holds when considering current noise, obviously referring to the current gain rather than to the voltage gain of the stages.

Noise Factor and Noise Figure. Noise factor F is one of the most traditional parameters used to characterize the noise performance of an amplifier. It is defined as the ratio of the total available output noise power per unit bandwidth to the portion of that output noise power caused by the noise associated with the sensor, measured at the standard temperature of 290 K (4). To emphasize that this parameter is a point function of frequency, the term "spot noise factor" may be used. Since the noise factor is a power ratio, it can be expressed in decibels. In this case, the ratio is referred to as noise figure (*NF*). That is, taking Fig. 2 and Eq. (3) into account,

$$\mathrm{NF} = 10 \cdot \log \frac{V_{n,o}^2}{V_{n,s}^2 \cdot |A_v'|^2} = 10 \cdot \log \frac{V_{n,eq}^2}{V_{n,s}^2} \quad (7)$$

An alternative expression for the noise figure can be derived from Eq. (7), obtaining

$$\begin{aligned} \mathrm{NF} &= 10 \cdot \log \frac{V_s^2 V_{n,o}^2}{V_{n,s}^2 \cdot (V_s^2 \cdot |A_v'|^2)} = 10 \cdot \log \frac{(V_s^2/V_{n,s}^2)}{(V_o^2/V_{n,o}^2)} \\ &= 10 \cdot \log \frac{(\mathrm{SNR})_i}{(\mathrm{SNR})_o} \end{aligned} \quad (8)$$

where $(\mathrm{SNR})_i$ is the signal-to-noise ratio (*SNR*) available at the sensor output, and $(\mathrm{SNR})_o$ is the SNR at the output of the real (i.e., noisy) amplifier. The above result indicates that NF accounts for the signal-to-noise power degradation caused by the preamplifier. Thus, for an ideal amplifier, which does not add any noise, the output signal-to-noise ratio is kept equal to its input counterpart, and NF = 0 dB. Alternatively, an NF of 3 dB means that half the output noise power is due to the amplifier.

As will be shown later, NF by itself is not always an appropriate figure of merit to characterize the noise performance of an amplifier. As stated above, NF is only valid to indicate how much noise is added by a preamplifier to a given input source resistance, and is therefore useful to compare noise behavior of different preamplifiers with a determined signal source. However, it is not a useful tool for predicting noise performance with an arbitrary source.

Noise Matching. Let us consider now the particular case where the internal impedance of the signal source is a resistor R_s. This corresponds to one of the most frequently used types of sensors, which can be represented by a signal source generator V_s in series with its internal resistance and a thermal noise generator $V_{n,s}$, whose power spectral density is:

$$V_{n,s}^2 = 4KTR_s \tag{9}$$

where K is Boltzmann's constant (1.38×10^{-23} Ws/K) and T is the absolute temperature (K). According to Eq. (7), the noise figure for this resistive signal source is given by

$$\mathrm{NF} = 10 \cdot \log \frac{4KTR_s + V_{n,a}^2 + I_{n,a}^2 R_s^2}{4KTR_s} \tag{10}$$

By differentiating this expression with respect to R_s, one obtains the so-called optimum source resistance, for which NF is minimum:

$$R_{opt} = \frac{V_{n,a}}{I_{n,a}} \tag{11}$$

From Eqs. (10) and (11), NF can be written as

$$\mathrm{NF} = 10 \cdot \log \left[1 + \frac{V_{n,a} \cdot I_{n,a}}{4KT} \left(M + \frac{1}{M} \right) \right] \tag{12}$$

in which $M = R_s/R_{opt}$ is the matching factor. For a given $V_{n,a} \cdot I_{n,a}$ product, NF is minimum for $M = 1$.

The effect of the source resistance variation on NF for amplifiers having different values of the noise sources product $V_{n,a} \cdot I_{n,a}$, is illustrated in Fig. 4 [p. 46 in Ref. 2.]. The minimum value of the noise figure, NF_{opt}, occurs at $R_s = \mathrm{R}_{opt}$. As the product $V_{n,a} \cdot I_{n,a}$ increases, the noise figure also increases and is more sensitive to source resistance variations.

In the more general case where the correlation factor, γ, is different from zero, the optimum value, F_{opt}, of the noise factor corresponding to the optimum source resistance is easily calculated as

$$F_{opt} = 1 + \frac{2 \cdot (1+\gamma) \cdot I_{n,a}^2 \cdot R_{s,opt}^2}{V_{n,s}^2} = 1 + \frac{(1+\gamma) \cdot I_{n,a} \cdot V_{n,a}}{2KT} \tag{13}$$

F_{opt} defines the best performance obtainable when the source resistance can be selected to match R_{opt}. Eq. (13) also clearly shows that, for any given source resistance and temperature, the best noise performance, obtained when perfect matching is achieved, depends on the product $V_{n,a} \cdot I_{n,a}$ of the amplifier (5,6).

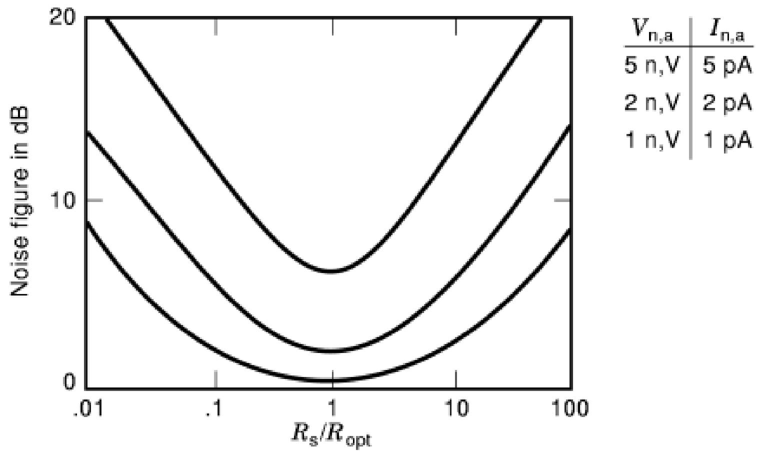

Fig. 4. NF reaches its minimum value for $R_s = R_{opt}$. NF increases with increasing value of the product $V_{n,a} \cdot I_{n,a}$.

Noise matching is based on the idea of modifying the amplifier equivalent input noise sources as seen at the signal source location, to meet the condition $R_s = R_{opt}$, so as to minimize the total equivalent input noise (5). This condition, which indicates that the preamplifier input stage is matched to the sensor, is considered as the essence of low-noise design. Of course, to keep the noise low, the rest of the amplifier must also be designed so that its noise contributions are low compared with those of the input stage.

A very simple and illustrative way to modify the amplifier equivalent input noise consists of coupling the sensor to the amplifier by means of a transformer with a primary-to-secondary turns ratio of 1:N (Fig. 5 shows this for the case of a resistive sensor). The amplifier noise sources are reflected to the primary as $V'_{n,a} = V_{n,a}/N$ and $I'_{n,a} = NI_{n,a}$. The ratio of these reflected parameters is:

$$R'_s = \frac{V'_{n,a}}{I'_{n,a}} = \frac{R_{opt}}{N^2} \tag{14}$$

Matching R'_s to R_s, one can derive the turns ratio required in the coupling transformer:

$$N = \sqrt{\frac{R_{opt}}{R_s}} \tag{15}$$

When this condition is met, the amplifier sees the optimum source resistance and, hence, the equivalent input noise is minimized. It has to be pointed out that a real transformer has its own internal noise sources and stray impedances, which have to be taken into account in an accurate low-noise design. Moreover, the use of a transformer requires a suitable shield to external electromagnetic fields, which can induce spurious currents in the transformer itself.

According to the above results, it appears that the noise figure NF can be alternatively improved by adding a series or shunt resistance to a given source resistance R_s (or, by correspondingly changing the sensor resistance), to make its final value equal to R_{opt}. However, due to the addition of an extra resistor, the signal-to-noise ratio gets worse. On the other hand, for $R_s = 0$, NF goes to infinity, although the actual output noise is less than that corresponding to any other value of source resistance, including R_{opt}. This contradictory situation arises from the fact that reducing NF improves the output SNR only if the SNR at the source remains constant.

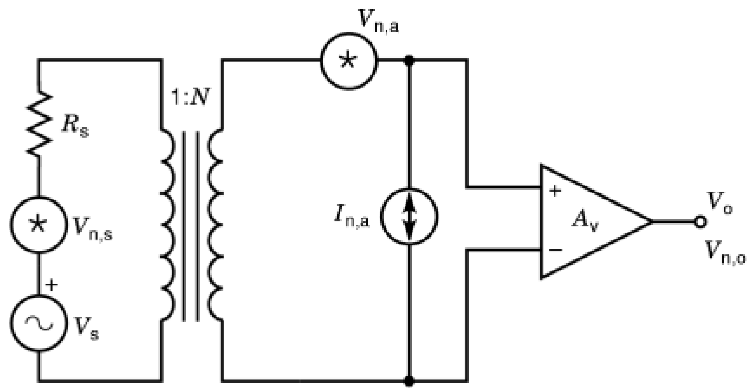

Fig. 5. Noise matching by coupling transformer minimizes the total equivalent input noise.

This condition is not met when matching is achieved by modifying the source resistance, but it is satisfied when using a coupling transformer. For the same reason, only when increasing sensor resistance increases the signal proportionally, it should be modified so as to match the amplifier optimum noise source resistance. When choosing or designing a preamplifier, the best noise performance is obtained by achieving the minimum equivalent input noise rather than the lowest noise figure.

Noise matching can also be achieved in the case of narrow-band signal sources. By exploiting the resonance of a suitable *LC* group, the amplifier equivalent input noise as seen at the signal source location, can be optimized at the required center frequency. It is possible to follow this approach for both resistive and reactive narrow-band sources (6).

Since transformers, as well as other coupling techniques using discrete components, are not compatible with solid-state circuits, noise matching for monolithic preamplifiers has to be obtained by appropriate choice of transistor sizes and bias conditions (7). In particular, when $V_{n,a}$ is the dominant noise source of the preamplifier, noise matching can be obtained by using n input transistors connected in parallel rather than a single input transistor. Indeed, this technique reduces input noise voltage by a factor of $\sqrt{n}$ and increases input noise current by the same factor, which from the noise standpoint, is equivalent to using a coupling transformer with a turns ratio of 1:$\sqrt{n}$ (5). Similar techniques can also be adopted for discrete preamplifiers, even though much less flexibility is obviously available.

Design Considerations for Preamplifiers

Designing or selecting a preamplifier for a specific application involves many specifications and choices. The procedure starts by considering sensor characteristics, such as signal source type, noise, impedance, and frequency response. As a function of that, the preamplifier must be designed so as to achieve the lowest value of equivalent input noise.

According to the above discussion, the ultimate limit of equivalent input noise is determined by the sensor impedance Z_s and the amplifier noise generators, $V_{n,a}$ and $I_{n,a}$, where all these parameters may generally be frequency dependent. Therefore, the signal source impedance and frequency range are decisive when choosing the type of preamplifier input device, as in a well-designed amplifier, noise performance is heavily affected by this element. To assist in this task, Fig. 6 [p. 210 in Ref. 2] can serve as a general guide. In this figure, the different ranges of source impedance values are covered by the different types of active or coupling devices. Low values of source resistance usually require the use of a coupling transformer for noise matching, while, for

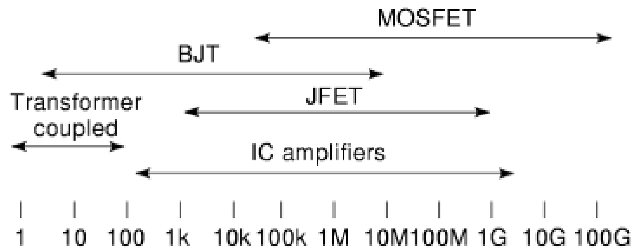

Fig. 6. Guide for selection of input devices.

matching the highest source resistance range, the extremely low noise current $I_{n,a}$ of field-effect transistors is exploited.

With respect to the frequency range, in the simplest case of a resistive source, matching the amplifier optimum source resistance R_{opt} to the source resistance, minimizes the equivalent input noise at a given frequency. However, if the preamplifier must operate over a large frequency band, the designer's task is to minimize the noise integrated over this interval. Then, if the source impedance is reactive and/or the equivalent amplifier noise sources are functions of frequency, the use of a circuit simulator is often necessary to perform this integration over the whole bandwidth and optimize noise performance. With respect to this, it is important to note that the preamplifier bandwidth has to match, as much as possible, the signal spectrum needed in the specified application, since increasing the bandwidth increases the integrated output noise. Once the low and high amplifier cutoff frequencies of the preamplifier have been adjusted, the computer analysis may show that noise requirements are not fullfilled and, then, another operating point or different device sizes must be chosen. In extreme cases, different amplifiers or circuit topologies must be used.

Finally, needless to say, any noise injection from external sources must be minimized. For example, in case electrical and/or magnetic shielding has to be provided against electromagnetic interference, power supply filtering can be required to ensure a quiet supply voltage, ground connections have to be carefully studied, noise injection from digital sections has to be minimized. However, these considerations regard general system design, and are not specific to preamplifier design.

Next, the above design considerations are particularized for three types of source impedances (i.e., resistive, capacitive, and inductive), with emphasis in amplifiers for monolithic implementations. For this reason, mainly bipolar and MOS transistors will be considered as amplifier devices.

Preamplifiers with Resistive Sources. The simplest type of source impedance is a resistance. Among sensors with this type of source impedance, some (i.e., voltaic sensors, such as thermocouples, thermopiles, infrared detectors, etc.) generate a voltage signal, while others (e.g., photoconductive detectors used in opto-electronic applications) produce a current signal. Figure 7 shows two generic preamplifiers with a resistive source (the noise sources, i.e., the resistor thermal noise generators and the equivalent amplifier input noise generators, are also included in both schemes). In Fig. 7(a), a sensor voltage source is coupled to a voltage amplifier by means of a coupling capacitor C_c, while a resistor R_b is added for biasing the amplifier input device, which corresponds to a very usual situation. Instead, a resistive sensor, which provides a current signal, has been assumed in Fig. 7(b). In this case, a transimpedance amplifier is used to amplify the signal from the high impedance source. The transimpedance gain of the amplifier, V_o/I_s, is determined by the feedback resistor R_f, provided that the loop gain is high enough.

Referring to the voltage amplifier in Fig. 7(a), a high-pass response is caused by the coupling capacitor C_c along with the equivalent series resistance of the input network. C_c must be chosen in such way that its reactance can be neglected in the frequency range of interest. Thus, the voltage gain in the input network is substantially independent of frequency. Moreover, the contribution of $I_{n,a}$ to the equivalent input noise voltage $V^2_{n,eq}$ [see Eq. (3)] results equal to $(I_{n,a}R_s)^2$.

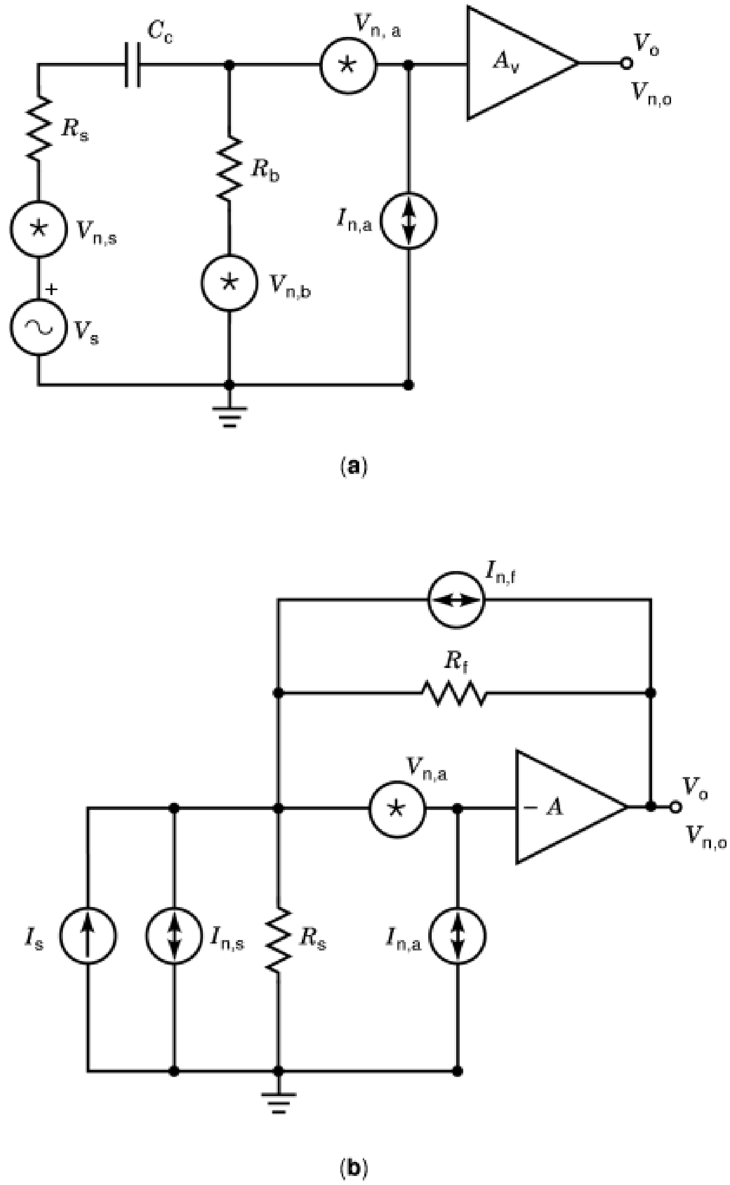

Fig. 7. Preamplifiers with resistive sources: (a) voltage amplifier with coupling capacitor; (b) wide-band transimpedance preamplifier.

Assuming a much higher amplifier input impedance than R_s and R_b, the equivalent input noise voltage of the system turns out to be:

$$\begin{aligned} V_{n,eq}^2 \cong {} & V_{n,s}^2 + V_{n,b}^2 \frac{R_s^2}{R_b^2} + V_{n,a}^2 \frac{(R_s + R_b)^2}{R_b^2} \\ & + I_{n,a}^2 \cdot R_s^2 + 2\gamma V_{n,a} I_{n,a} (R_s + R_b) \frac{R_s}{R_b} \end{aligned} \tag{16}$$

In the remainder of this article, the generally accepted assumption that the amplifier noise is dominated by its input device will be adopted. In addition, single-ended input stages, which as a general rule allow the designer to minimize the noise contribution of the amplifier, will also be assumed.

First consider the case when the input transistor is a bipolar device. Neglecting 1/*f* noise and frequency-dependent terms in the frequency band of interest, the equivalent input noise sources can be approximated as (6):

$$V^2_{\mathrm{n,a}} = 4KTr_{\mathrm{b}} + \frac{2\cdot(KT)^2}{qI_{\mathrm{E}}} \tag{17a}$$

$$I^2_{\mathrm{n,a}} = 2qI_{\mathrm{B}} = 2q\frac{I_{\mathrm{C}}}{\beta} \tag{17b}$$

where r_{b} is the base resistance, q is the electron charge, I_{E}, I_{B}, and I_{C} are the dc emitter, base and collector currents, respectively, and $\beta = I_{\mathrm{C}}/I_{\mathrm{B}}$ is the dc current gain. This operating region of the BJT is known as *shot noise region* (2), since the shot noise mechanisms are the dominant ones. In this operating region, the correlation effects between the input voltage and current noise sources can be usually neglected ($\gamma \cong 0$). Here and in the following, it shall also be assumed that the noise contribution by the base resistance is negligible, as can be achieved with adequate layout, that is by making r_{b} sufficiently small. The optimum noise resistance can be expressed as a function of the design parameters of the input transistor:

$$R_{\mathrm{opt}} = \frac{V_{\mathrm{n,a}}}{I_{\mathrm{n,a}}} \cong \frac{KT}{qI_{\mathrm{C}}}\sqrt{\beta} \tag{18}$$

The equivalent input noise of the system is minimum when the noise matching condition is fulfilled, that is when R_{opt} as from Eq. (18) is made equal to the equivalent resistance of the input network, $R_{\mathrm{s}} \| R_{\mathrm{b}}$. This is achieved for the following biasing collector current:

$$I_{\mathrm{C,opt}} = \frac{KT}{q}\frac{1}{(R_{\mathrm{s}}\|R_{\mathrm{b}})}\sqrt{\beta} \tag{19}$$

Obviously, the same result is achieved by differentiating $V_{\mathrm{n,eq}}$ with respect to I_{C} for $V_{\mathrm{n,eq}}$, as given by Eq. (16).

Replacing Eq. (19) into Eq. (16), the total equivalent input noise for the optimum biasing collector current can be derived:

$$V^2_{\mathrm{n,eq}} = 4KTR_{\mathrm{s}}\left(1+\frac{R_{\mathrm{s}}}{R_{\mathrm{b}}}\right)\cdot\left(1+\frac{1}{\sqrt{\beta}}\right) \tag{20}$$

The first term, $4KTR_{\mathrm{s}}(1 + R_{\mathrm{s}}/R_{\mathrm{b}})$, is due to the thermal noise contribution of the source and biasing resistances, while the second term, $4KTR_{\mathrm{s}}(1 + R_{\mathrm{s}}/R_{\mathrm{b}})\beta^{-1/2}$, arises from the amplifier noise. It is apparent that the noise contributed by the amplifier is lower than the thermal noise by a factor of $\beta^{1/2}$. Also, the noise contribution of the biasing resistor can always be kept lower than that of R_{s}, by choosing $R_{\mathrm{b}} > R_{\mathrm{s}}$. Therefore, the noise performance of voltage amplifiers with bipolar input devices and resistive sources can be made to be dominated by the resistive source itself, if I_{C} can be chosen equal to $I_{\mathrm{C,opt}}$. An alternative interpretation of Eq. (19) consists in considering the term $(1 + \beta^{-1/2})$ as the factor by which the preamplifier increases the thermal noise of the source and biasing resistances. In other words, this term is the lowest value of the optimum noise factor, F_{opt}, of a BJT working in the shot noise region used as the input device of an amplifier, which is obtained when the value of $I_{C,opt}$ corresponds to a sufficiently small collector current density (2).

Very similar conclusions are obtained when considering transimpedance amplifiers with resistive sources (3)—see Fig. 7(b). Following the above procedure, one finds that the bias collector current of the input bipolar transistor for minimum noise is $I_{C,opt} = (KT/q)\beta^{1/2}/(R_s \| R_f)$, and that the corresponding total equivalent input noise current is $I^2_{n,eq} = [4KT/(R_s \| R_f)] \cdot (1 + \beta^{-1/2})$. Again, in a well-designed bipolar preamplifier, noise performance can be made to be dominated by the resistive source, if R_f can be chosen sufficiently large. The choice of the feedback resistor R_f will result as the best trade-off between noise, transimpedance gain, and bandwidth requirements.

Now refer to the case when an MOS transistor is used as the input device of the preamplifier in Fig. 7(a). The equivalent input noise generators of an MOS device in the mid-frequency range can be approximated as (3):

$$V^2_{n,a} = \frac{8}{3}\frac{KT}{g_m} + \frac{A_f}{WLf} \tag{21a}$$

$$I^2_{n,a} = |j\omega C_i|^2 V^2_{n,a} \tag{21b}$$

where A_f is a suitable technology-dependent constant, W and L are the width and length, respectively, of the transistor, g_m is its transconductance, and C_i its input capacitance. As the noise voltage source is placed in series with the signal source, the only way to minimize its contribution to the total equivalent input noise voltage $V^2_{n,eq}$ is to minimize the noise source itself. To reduce thermal noise, a large transistor transconductance must be used, which means a large aspect ratio and a large bias current. To reduce the $1/f$ term, a large gate area is required. The contribution of the noise current source to $V^2_{n,eq}$ is equal to $V^2_{n,a}[\omega(R_s \| R_b)C_i]^2$, and is, therefore, negligible with respect to $V^2_{n,a}$ in the frequency band of interest $\{\omega < [(R_s \| R_b)C_i]^{-1}\}$.

When transimpedance amplifiers in MOS technology are considered, the contribution of the term $V^2_{n,a}$ to the total equivalent input noise current is given by $V^2_{n,a}/(R_s \| R_f)^2$. This should be compared with the noise current $4KT/(R_s \| R_f)$ contributed by the source and feedback resistances. Therefore, in the presence of a very large source resistance, the noise contribution of the amplifier can be made negligible provided that a sufficiently large feedback resistor is used. In this case, MOS amplifiers should be preferred to bipolar ones (3). By contrast, in the case of a small source resistance, the source $V^2_{n,a}$ must be minimized to ensure low-noise performance of the preamplifier. This can be obtained with the same techniques as seen above for the case of the voltage amplifier. Again, the contribution due to the amplifier input current noise can be neglected in the frequency band of interest.

Preamplifiers for Optical Receivers. A very popular preamplifier application is for optical receivers. An optical receiver is a circuit able to detect and process a signal coming from an optical source. Basically, it is made up of an optical sensor followed by a preamplifier and a processing section. The optical sensor (photodetector), which in its simplest form, is a reversed-biased diode, converts the optical signal into an electrical current. The photodetector is modeled as a current source with an ideally infinite output resistance and a capacitance in parallel. As the input electrical signal can be very small (e.g., down to the nA range), it must be amplified with a preamplifier to a level suitable for the following processing. Therefore, low noise, high gain and, in many cases, high bandwidth and adequate dynamic range, are key amplifier requirements in this kind of application.

The basic principle of a preamplifier for optical receivers is to convert the current signal provided by the photodetector, I_s, into a voltage signal having a suitable amplitude. The most popular configuration consists of a transresistance amplifier, as illustrated schematically in Fig. 8(a) (8), where noise generators are not shown. The current I_s generated by the photodetector flows through the feedback resistor R_f which, in turn, produces an amplifier output voltage $V_o = -I_s R_f$, provided that the loop gain is large enough. The required current-to-

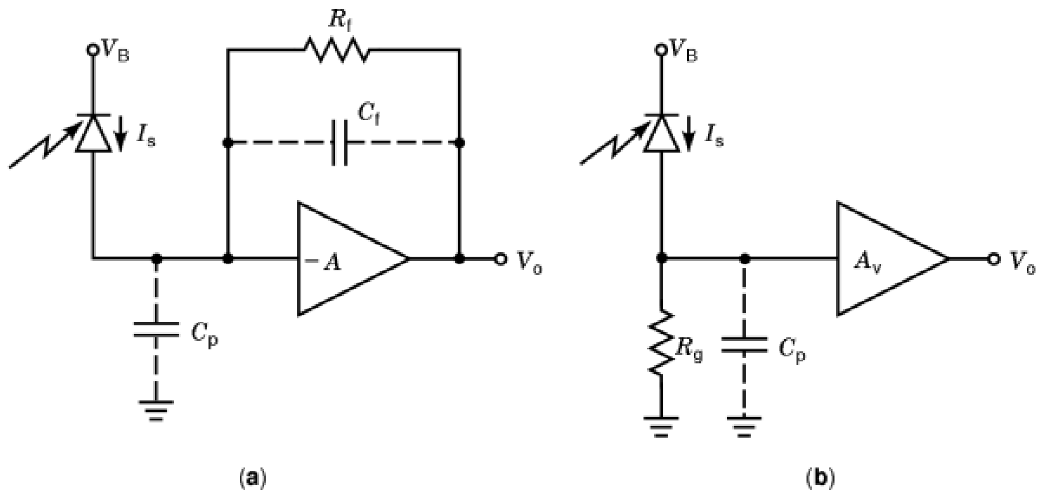

Fig. 8. Preamplifiers for optical receivers: a transresistance preamplifier (a) is generally preferred to the use of a grounded resistor followed by an active stage (b).

voltage conversion can also be achieved by feeding the signal current directly to a grounded resistor R_g [Fig. 8(b)] (9). A suitable active stage is cascaded to provide decoupling between the input section and the following stages and, in this case, additional voltage gain. The choice of R_g results as a tradeoff between gain (V_o/I_s) and low thermal noise added to the signal current ($4KT/R_g$) on the one hand, and bandwidth, which is limited to $1/(2\pi R_g C_p)$, on the other, where C_p includes the photodetector capacitance in parallel with the amplifier input capacitance. For this reason, an equalizer stage (substantially, a parallel group RC) is very often cascaded to the active stage when R_g has a large value (9). The use of a large R_g also causes a limited input dynamic range, as the whole voltage signal $R_g I_s$, is applied to the input of the active stage.

The transresistance configuration of Fig. 8(a) provides the best trade-off in terms of noise and gain on the one hand and bandwidth on the other, and also gives no problems regarding input dynamic range. The achievable signal bandwidth (assuming that the amplifier has an ideal frequency behavior) is now equal to $1/[2\pi R_f(C_f + C_p/A)]$, where C_f is the parasitic capacitance around the amplifier ($C_f \ll C_p$). The actual bandwidth of the system is limited either by parasitic capacitances in the feedback network or by the bandwidth of the amplifier. The former is a common case in high-gain applications, when a large value of R_f is used, while the latter is more typical in lower-gain applications. In any case, attention must be paid to achieving frequency stability, as a closed-loop configuration is adopted. Neglecting the feedback parasitic capacitance, the equivalent input current noise of the system in the frequency band of interest is

$$I_{n,eq}^2 = 4\frac{KT}{R_f} + I_{n,s}^2 + I_{n,d}^2 + I_{n,a}^2 + V_{n,a}^2\left|\frac{1+\omega R_f C_p}{R_f}\right| \qquad (22)$$

where $I_{n,s}$ and $I_{n,d}$ account for shot noise of signal and dark currents of the photodetector, respectively. From the above equation, one can observe that the contribution of $V_{n,a}$ to the total equivalent input noise increases at high frequencies, even though at low frequencies, it can be negligible if $V_{n,a}$ is sufficiently small ["noise gain peaking" effect (8)]. However, at very high frequencies, the contribution of $V_{n,a}$ is limited by the ratio C_p/C_f and then rolls off due to the amplifier open-loop response.

Preamplifiers with Capacitive Sources. A capacitive sensor source can be modeled, in its useful frequency range, as a voltage source in series with a capacitor or as a current source in parallel with a capacitor (the case where the sensor signal is delivered in the form of a charge packet will be briefly addressed at the end of this section). The output signal of the sensor is taken either as the open-circuit voltage or the short-circuit current, respectively. Sensor capacitance and signal frequency depend on the application, and can vary by several orders of magnitude (from picofarad up to nanofarad and from hertz to megahertz ranges, respectively). Typical examples are capacitive antennas (e.g., for radio receivers), electret microphones, some piezoelectric sensors such as hydrophones, optical detectors, and so forth. In this section, wide-band monolithic preamplifiers, specifically, will be considered. In the case of narrow-band applications, noise optimization can be achieved by adding a suitable series or parallel inductance in the input network, using a technique very similar to that used for narrow-band preamplifiers with inductive sources (6) (see the next section). The basic principle is to determine a proper resonance which ideally makes the effects of the amplifier input current or voltage noise source disappear at the frequency of interest, thereby minimizing the system equivalent input noise.

Two basic topologies of wide-band preamplifiers for capacitive signal sources are depicted in Fig. 9, where the voltage source representation is used for the sensor, and equivalent input noise generators are also shown. Notice that, ideally, no noise is generated in the signal source, due to its reactive nature. In Fig. 9(a), a biasing resistor R_b has been included. This resistor must be large enough so that, in the frequency band of interest, the pole generated by the group R_bC_c roughly cancels out the effects of the zero located in the origin, which arises due to C_c. Thus, the preamplifier gain is independent of frequency, as required in most wide-band applications. This is a typical situation in preamplifiers for electret microphones, where, in the case of monolithic implementations, an active biasing resistor is generally used to avoid excessive silicon area occupation due to the large resistance value required (10,11). Noise considerations for this topology are very similar to those for voltage amplifiers with resistive sources, although in the present case the source resistance is assumed to be negligible, and obviously the dominant noise source is the amplifier.

In the capacitive-feedback structure of Fig. 9(b), no dc feedback or biasing element has been drawn, although generally dc stabilization is required (this can be obtained, e.g., with a very large feedback resistor, and will be neglected in the following noise considerations). In this scheme, the feedback capacitor C_f sets the mid-frequency voltage gain equal to $-C_s/C_f$. Also in this case, therefore, the gain is substantially independent of frequency. Moreover, it shows no dependence upon the parasitic capacitance C_p associated to the input line, which is very useful in applications requiring long cable connections between the sensor and the amplifier (12). Choosing the best value of C_f derives from two contrasting requirements. On the one hand, a small capacitor C_f should be chosen, so that the minimum input signal must be amplified to a level adequate to drive the cascaded stages, while on the other hand, capacitor C_f should not be so small that the amplifier output saturates in the presence of the maximum allowed input signal.

Again, regardless of the application, the noise performance of the preamplifier is of paramount importance, as it generally determines the sensitivity of the overall system. From Fig. 9(b), the equivalent input noise voltage is

$$
\begin{aligned}
V_{n,eq}^2 = {} & V_{n,a}^2 \left[\frac{C_f + C_s + C_p}{C_s}\right]^2 + I_{n,a}^2 \left|\frac{1}{j\omega C_s}\right|^2 \\
& + 2\gamma \left|V_{n,a} I_{n,a} \frac{1}{j\omega C_s}\right| \frac{C_f + C_s + C_p}{C_s}
\end{aligned}
\tag{23}
$$

For the best noise performance, the most straightforward choice is again the use of single-ended input stages, although fully differential amplifier solutions are also used for this kind of sensors (12,13). As pointed out above, in this section we consider mainly bipolar and MOS input devices, as currently JFET circuits are used only in specific applications (e.g., in charge-sensitive amplifiers for nuclear physics experiments; see below). In the case of a bipolar input transistor, taking into account its equivalent input sources given in Eqs. (17) and

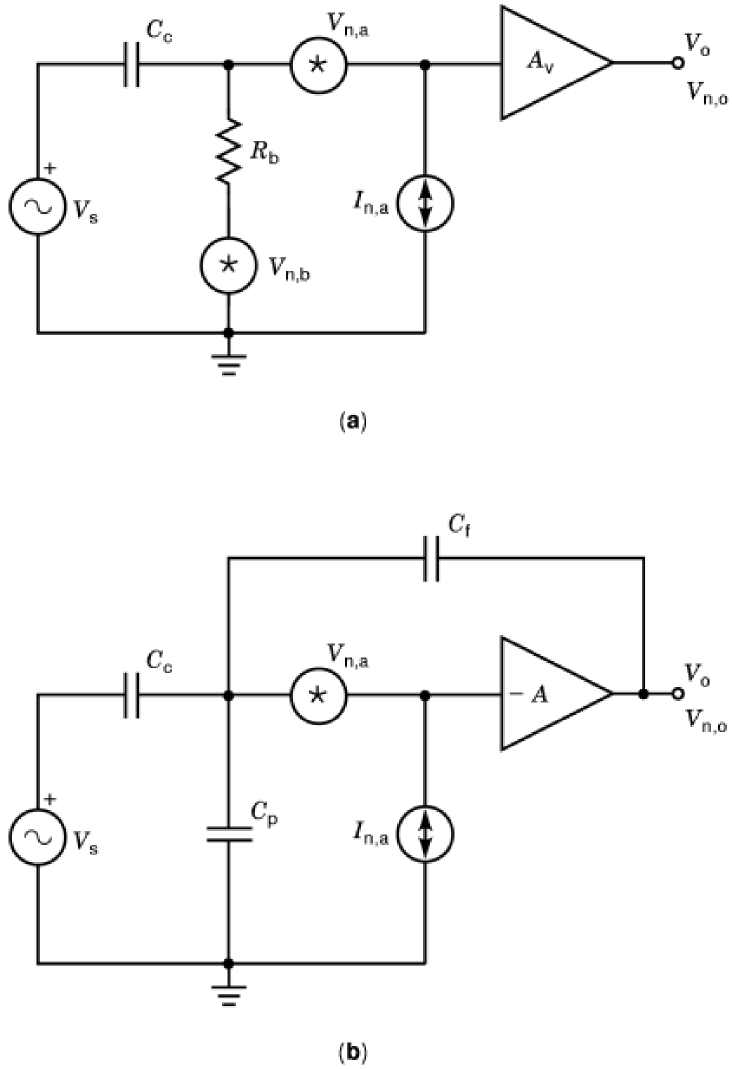

Fig. 9. Preamplifier with capacitive sources: (a) voltage amplifier with biasing resistor; (b) voltage amplifier with capacitive feedback.

neglecting the correlation factor γ, the total equivalent input noise turns out to be:

$$V_{\mathrm{n,eq}}^2 = 4KT\left(r_{\mathrm{b}} + \frac{KT}{2qI_{\mathrm{C}}}\right)\cdot\left(\frac{C_{\mathrm{f}} + C_{\mathrm{s}} + C_{\mathrm{p}}}{C_{\mathrm{s}}}\right)^2 + \left(\frac{2qI_{\mathrm{C}}}{\beta}\right)\left|\frac{1}{j\omega C_{\mathrm{s}}}\right|^2 \tag{24}$$

It is apparent that a small base resistance r_{b} and a high large current gain β are needed for low noise. Moreover, one can see that, for any given value of I_{C}, the base current shot-noise contribution [second term in Eq. (24)] is dominant at low frequencies, while voltage noise [first term in Eq. (24)] dominates at high frequencies. To achieve noise minimization, noise matching must be achieved by a suitable choice of the collector bias current

I_C. Indeed, increasing I_C has opposite effects on the two noise contributions. The optimal value of I_C can be easily calculated by taking the derivative of Eq. (24) with respect to I_C, obtaining (3,7):

$$I_{C,opt} = \frac{KT}{q}\omega(C_s + C_p + C_f)\sqrt{\beta} \tag{25}$$

Notice that Eq. (25) is formally identical to Eq. (19): $\omega(C_s + C_p + C_f)$ represents the module of the admittance to the input network. As observed, $I_{C,opt}$ depends on the frequency. As a consequence, when required, wide-band noise optimization with bipolar input stages is not possible. Obviously, when choosing the value of I_C, other features such as gain and operation speed must also be taken into account.

In the case of an MOS input transistor, using the noise sources in Eqs. (21), the equivalent input voltage noise source turns out to be:

$$V^2_{n,eq} = V^2_{n,a}\left[\frac{C_f + C_s + C_p + C_i}{C_s}\right]^2 \tag{26}$$

where the term C_i results from the presence of the input noise current, taking also in account the 100% correlation existing between $V_{n,a}$ and $I_{n,a}$.

It should be emphasized that noise transfer gain does not depend on frequency. The term $V^2{}_{n,a}$ includes a flicker as well as a thermal component. Both these contributions should be reduced to a minimum to achieve low-noise performance. To reduce input-referred noise, capacitances C_p and C_f must be minimized, even though they are noiseless elements. As far as C_i is concerned, it is worth pointing out that its value is strictly related to the input transistor size. Changing its value has two opposite effects on noise performance. On the one hand, increasing the aspect ratio *W*/*L* of the input device leads to a decrease in both flicker and thermal noise, as a result of the corresponding increase in its gate capacitance and transconductance, respectively. On the other, from Eq. (26), increasing C_i will also degrade noise performance. An optimized value of the input transistor capacitance and, hence, of its size, is therefore necessary, which is determined by taking the derivative of Eq. (26) with respect to C_i. The gate length should be set to the minimum to maximize amplifier performance in terms of thermal noise and gain-bandwidth product. Noise optimization results are different when flicker and thermal components are considered, as a consequence of the different dependence of their noise spectral density upon C_i. In the case of flicker noise, the best capacitance matching is obtained by setting $C_i = C_s + C_p + C_f$, while for thermal noise, the best value is $C_i = (C_s + C_p + C_f)/3$. When both flicker and thermal noise contributions are important, a trade-off value of C_i is chosen, for example, the average of the two optimal values (3). An analytical derivation of the optimum C_i value in the presence of both thermal and flicker series noise can be found in (14). A suitably large bias current is also required to maximize the transconductance of the input transistor and, hence, reduce its thermal noise. An *n*-channel input device also helps to this end. On the contrary, flicker noise is generally smaller for *p*-channel devices (15,16,17).

It has been shown (3) that, for a capacitive source, an MOS input device offers better noise performance than a bipolar one. Obviously, a suitable design is needed to minimize noise contributions by the other components and following stages in the circuit (for the latter purpose, e.g., some gain should be introduced in the first stage of the amplifier). Depending on the application, high linearity, large load drive capability, and wide output dynamic range can also be required of the preamplifier, these features being related mainly to an optimized design of its output stage. Moreover, due to the presence of the feedback loop, adequate frequency stability must be provided. Bipolar technology offers inherent advantages for such requirements, however, CMOS preamplifiers meeting all the specifications needed can be developed using adequate circuit design approaches. These include using a three-stage topology, a noninverting class A-B output stage, and suitable compensation techniques (3),

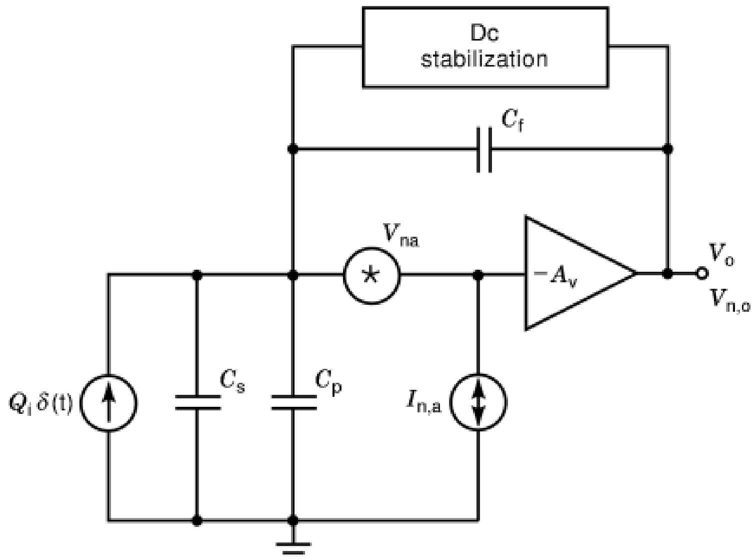

Fig. 10. Basic scheme of a charge-sensitive preamplifier.

and employing parasitic bipolar transistors (12). When possible, CMOS technology is the preferred choice as it allows the designer to integrate the preamplifier together with the cascaded processing section at low cost.

BiCMOS technology has also been proposed to implement the preamplifier (3). BiCMOS technology provides both CMOS and bipolar devices on the same chip. This allows the designer to take advantage of the superior noise performance of a CMOS transistor used as the input device and, at the same time, to exploit the excellent features of bipolar transistors to achieve the other requirements with simpler circuits with respect to fully CMOS solutions. The main disadvantage of BiCMOS technology is its increased process complexity and, hence, its higher cost.

Charge-Sensitive Preamplifiers. In some very important applications using a capacitive source, the input signal is delivered as a charge packet Q_i. The signal source can be generally represented as a delta-like current source $Q_i\delta(t)$. Popular examples are detector systems for elementary-particle physics experiments (18,19) and spectrophotometers and vision systems based on photodiodes operating in the storage mode (20). The basic scheme (Fig. 10) is substantially the same as the previous one. The readout amplifier, generally referred to as a *charge-sensitive amplifier,* produces an output voltage step with an amplitude equal to $-Q_iC_f$ in response to an input charge packet Q_i; dc stabilization is generally obtained either with a very large feedback resistor or with a feedback switch S_R, which is turned on during suitable reset time intervals.

The above noise-matching considerations still apply (in particular, the relationships obtained for the optimal input capacitance of the amplifier). In these applications, noise performance is usually expressed in terms of equivalent noise charge (*ENC*). This is defined as the charge which the detector must deliver to the amplifier input in order to achieve unity signal-to-noise ratio at the output, and is usually expressed in electrons.

Detectors for nuclear physics experiments represent a very critical application of charge-sensitive amplifiers. Here, the amplifier is generally followed by a noise-shaping filter (or "pulse shaper"), which has the purpose of optimizing the overall signal-to-noise ratio of the detector system. This is required as, in general, electronic noise sets the limit to the accuracy of these systems. The best achievable value of ENC increases, with a substantially linear relationship, with increasing detector capacitance C_s (in fact, a larger C_s leads to a larger equivalent noise charge for the same equivalent input noise). The obtained values of ENC ranges from few electrons for $C_s < 1$ pF (pixel detectors), to hundreds of electrons for microstrip detectors, up to thousands of electrons for calorimeter detectors (C_s in the order of several hundred or even more than 1000 pF).

In some applications, junction field-effect transistors (*JFET*) are preferred in front-end electronics for ionization detectors of capacitive nature, mainly because they show better radiation tolerance with respect to MOS devices and much smaller input current as compared to BJTs (21,22). Nevertheless, under particular operating conditions, such as very short shaping time (<50 ns) and low-power constraints, BJTs can offer superior performance (23,24). CMOS solutions have also been developed for readout electronics to exploit the capability of CMOS technology for very high integration density and low power consumption (3,25). In fact, as a huge number of read-out channels are needed in modern detector systems, small size and low power dissipation are also important requirements, which make the monolithic approach the most appealing solution. CMOS technology is very attractive, especially for detectors that are placed not very close to the radiation environment and use a pulse shaper with a very fast response (i.e., short peaking time), so that flicker noise is negligible with respect to thermal noise. A BiCMOS solution implementing a low-power high-gain transresistance amplifier has also been presented (26).

Preamplifiers for Inductive Sources. An inductive sensor source can be generally modeled as a current source in parallel with an inductance. An internal resistance can also be present, to account for the real part of the sensor impedance. Examples of inductive sensors include magnetic heads (e.g., for tape and video cassette recorders), inductive pick-ups, dynamic microphones, ferrite antennas, and so forth. The operation principle of such sensors is to convert the information, received in the form of an electromagnetic field, into an electrical signal by means of an inductive coil. In most cases, very weak signals are generated and, therefore, very severe noise specifications have to be met by the preamplifier. Obviously, the reactive elements in the circuit do not contribute any noise directly, however, their presence affects the noise behavior of the circuit.

Very different situations occur when narrow-band and wide-band applications are considered. A typical preamplifier topology for narrow-band inductive signal sources is illustrated in Fig. 11, where equivalent input noise generators are also shown. L_p is the source inductance, R_s is the sensor resistance, R_b can be a biasing or a load resistor, and C_p is a shunt capacitance (including both parasitic and, in this case, added capacitances). C_c is a dc decoupling capacitor ($C_c \gg C_p$), and will be regarded as a short circuit in the frequency band of interest. The voltage signal at the amplifier input turns out to be equal to:

$$V_i = \frac{I_s \cdot j\omega L_p R_T}{j\omega L_p + (1 - \omega^2 L_p C_p) R_T} \tag{27}$$

where $R_T = R_b \| R_s$. The presence of the resonance due to the group $L_p C_p$ is apparent.

For this configuration, one can choose a suitable size of the shunt capacitance C_p to obtain the best noise matching (6). In fact, the expression of the equivalent input noise current for the circuit in Fig. 11 is easily calculated as:

$$\begin{aligned} I^2_{n,eq} = I^2_{n,s} + I^2_{n,b} + I^2_{n,a} + V^2_{n,a}\left|\frac{1}{R_T} + \frac{1 - \omega^2 L_p C_p}{j\omega L_p}\right|^2 \\ + 2\mathrm{Re}\left\{I^*_{n,a} V_{n,a}\left(\frac{1}{R_T} + \frac{1 - \omega^2 L_p C_p}{j\omega L_p}\right)\right\} \end{aligned} \tag{28}$$

Each noise current source reflects unchanged to the input at any frequency. By contrast, the coefficient of the noise voltage contribution is frequency dependent, and turns out to be minimum at the resonant frequency $\omega_o = 1/(L_p C_p)^{1/2}$. This behavior obviously derives from the large impedance shown by the parallel group $L_p C_p$

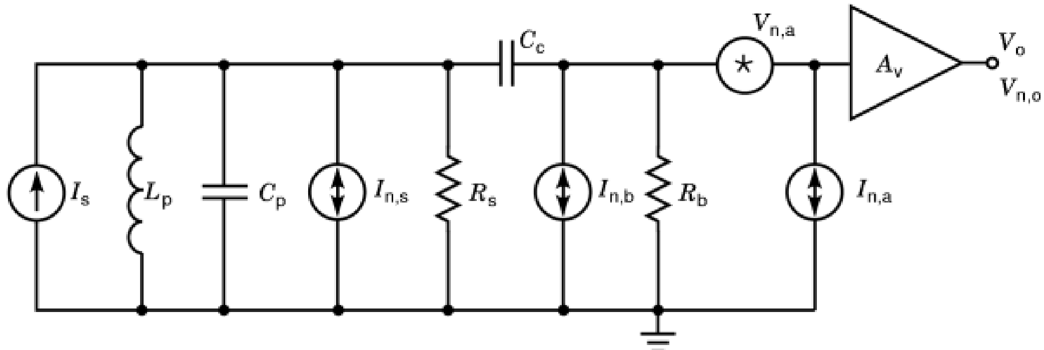

Fig. 11. Basic topology of a preamplifier for a narrow-band inductive source (shunt capacitance C_p includes both parasitic and, in this case, added capacitances).

at the resonance frequency. Neglecting the correlation effect between $V_{n,a}$ and $I_{n,a}$, the resulting equivalent input noise current is given by $I^2_{n,eq} = I^2_{n,s} + I^2_{n,b} + I^2_{n,a} + V^2_{n,a}/R^2_T$. It should be pointed out that no reactive element appears in the expression for minimum noise.

Let us now turn our attention to wide-band applications, where a flat response is required for the signal. The amplifier configuration in Fig. 11 can no longer be used, as the resonant group inherently provides narrow-band signal response. To overcome this limitation, a constant transimpedance topology can be used, as shown in Fig. 12. The voltage across the group L_pC_p is ideally maintained constant, regardless of signal amplitude and frequency, thereby preventing any resonance effect. The current I_s delivered by the sensor is injected into R_f, thus achieving the desired frequency-independent transfer gain: $V_o/I_s = -R_f$. The equivalent input noise current in this topology turns out to be:

$$\begin{aligned} I^2_{n,eq} = I^2_{n,s} + I^2_{n,f} + I^2_{n,a} + V^2_{n,a}\left|\frac{1}{R_s} + \frac{1}{R_f} + \frac{1-\omega^2 L_p C_p}{j\omega L_p}\right|^2 \\ + 2\mathrm{Re}\left\{I^*_{n,a}V_{n,a}\left(\frac{1}{R_s} + \frac{1}{R_f} + \frac{1-\omega^2 L_p C_p}{j\omega L_p}\right)\right\} \end{aligned} \tag{29}$$

The noise contributed by the amplifier is represented by the terms including $I_{n,a}$ and $V_{n,a}$. The use of a large inductance L_p reduces the contribution of $V^2_{n,a}$. This is especially true at low frequencies, where $\omega^2 L_p C_p \ll 1$. By contrast, at high frequencies, a small value of C_p helps to achieve low noise.

For practical cases, when very low noise is required, the term $I^2_{n,f} = 4KT/R_f$ due to the feedback resistor can result too high, thus setting too large a noise floor to the structure. To reduce this contribution, a combined capacitive and resistive feedback configuration has been proposed, as shown in Fig. 13 (27). The transimpedance gain of this structure is equal to $-[1 + j\omega(C_1 + C_2)R_f]/j\omega C_1$, which for the frequency range $\omega \gg 1/[(C_1 + C_2)R_f]$ can be approximated by $-R_f(C_1 + C_2)/C_1$ and, hence, achieves the required frequency independence. Obviously, a careful stability analysis is required when designing the amplifier for this feedback configuration. The input-referred noise current due to the feedback network turns out to be $I^2_{n,f}[C_1/(C_1 + C_2)]^2$, and is, therefore, reduced by a factor of $(1 + C_2/C_1)^2$, with respect to the noise generated by the feedback resistor. To obtain a substantial noise reduction, C_2 is set much larger than C_1 and, hence, the reduction factor becomes $\sim(C_2/C_1)^2$. In practice, to achieve any given transimpedance gain, we now use a resistor which is C_2/C_1 times smaller than in the case of a conventional transimpedance topology using a purely resistive feedback. Its current noise $I^2_{n,f}$ is, therefore, larger by the same factor, however, its input-referred contribution is divided by a factor of $(C_2/C_1)^2$

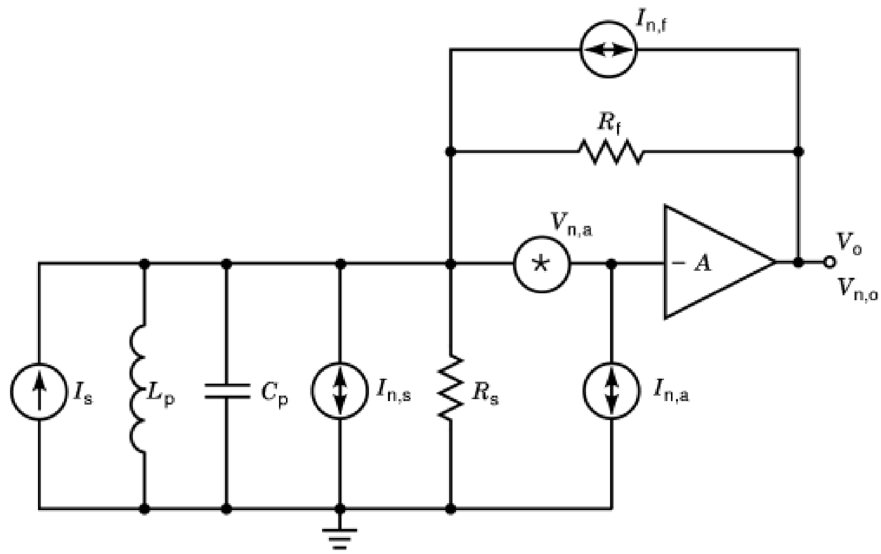

Fig. 12. A transimpedance configuration for an inductive source ensures frequency-independent gain.

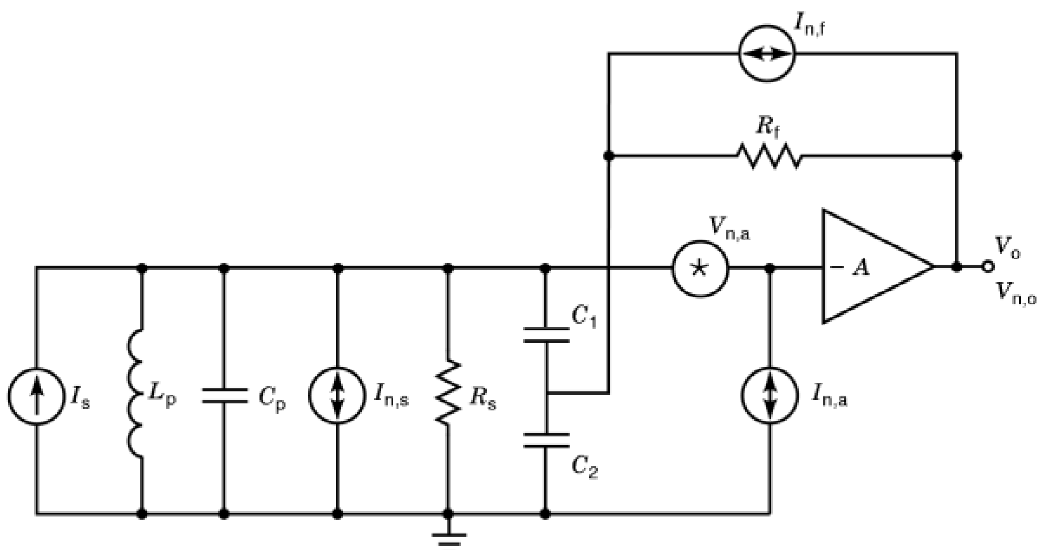

Fig. 13. The use of a combined resistive and capacitive feedback in a transimpedance amplifier minimizes the noise contribution of the feedback network.

and, therefore, a substantial improvement (by a factor of C_2/C_1) is achieved. It should be noted that with this assumption ($C_2 \gg C_1$), the resonance frequency in the input network is approximately equal to $\omega_{LC} = 1/[L_p(C_p + C_1)]^{1/2}$.

When a bipolar input transistor is used in the amplifier, the correlation term in Eq. (29) can be neglected, and noise minimization requires a small base resistance r_b and a large current gain β. Moreover, as in the case of a capacitive signal source, the collector current I_C must be set to an optimal value, as a consequence of its opposite effects on input voltage and current noise components. Again, this optimal current is frequency dependent, and therefore noise optimization cannot be obtained in a wide frequency range (3,27), leading to the choice of a trade-off current for any given application.

When using CMOS technology, no noise contribution due to the gate current is present, thus removing the basic limiting factor to the noise performance in bipolar preamplifiers (i.e., the base shot noise component). As for the case of capacitive signal sources, it can be shown that noise optimization is achieved by suitably sizing the input transistor of the preamplifier. Again, the optimal size is different when considering flicker and thermal noise. Furthermore, as a consequence of the frequency dependence of the coefficient of ${V^2}_{\mathrm{n,a}}$ in the expression of the total equivalent input noise current [see Eq. (29)], the optimal transistor size also depends on frequency, in contrast with the case of preamplifiers for capacitive sources. For frequencies much lower than the resonance frequency ω_{LC}, optimization is achieved by choosing an amplifier input capacitance $C_i \cong 1/(\omega^2 L_{\mathrm{p}})$ for both flicker and thermal noise (3). For $\omega > \omega_{\mathrm{LC}}$, wide-band noise optimization can be obtained by setting $C_{\mathrm{i}} = \sim(C_{\mathrm{P}} + C_1)/3$ and $C_{\mathrm{i}} = \sim(C_{\mathrm{P}} + C_1)$ in the thermal and flicker noise domain, respectively. Both noise components must be taken into account when determining the input transistor size for any given application, which can be done by using numerical simulation.

Also in the case of wide-band preamplifiers for inductive sources, a detailed noise analysis (3) shows that, in spite of the presence of a large flicker noise component, CMOS technology leads to better noise performance than the bipolar one. Again, BiCMOS technology has been proposed to exploit the advantages coming from integrating both CMOS and bipolar devices in the same chip, even though at an increased cost of the fabrication process.

BIBLIOGRAPHY

1. IRE Subcommittee 7.9 on Noise, Representation of noise in linear two ports, *Proc. IRE*, **48**: 69–74, 1960.
2. C. D. Motchenbacher J. A. Connelly *Low-Noise Electronic System Design*, New York: Wiley, 1993.
3. Z. Y. Chang W. M. C. Sansen *Low-Noise Wide-Band Amplifiers in Bipolar and CMOS Technologies*, Norwell, MA: Kluwer, 1991.
4. IRE Subcommittee on Noise, IRE standards on methods of measuring noise in linear two ports, 1959 (IRE Standard 59 IRE 20. S1), *Proc. IRE*, 48: 60–68, 1960.
5. Y. Netzer A new interpretation of noise reduction by matching, *Proc. IEEE*, **62**: 404–406, 1974.
6. Y. Netzer The design of low-noise amplifiers, *Proc. IEEE*, **69**: 728–741, 1981.
7. M. Steyaert Z. Y. Chang W. Sansen Low-noise monolithic amplifier design: Bipolar versus CMOS, *Analog Integr. Circuits Signal Process.*, **1**: 9–19, 1991.
8. J. G. Graeme *Photodiode Amplifiers: Opamp Solutions*, New York: McGraw-Hill, 1996.
9. D. J. T. Heatley Optical Receivers, in J. E. Franca and Y. Tsividis (eds.), *Design of Analog-Digital VLSI Circuits for Telecommunications and Signal Processing*, 2nd ed., Englewood Cliffs, NJ: Prentice-Hall, 1994.
10. J. Silva-Martínez J. Salcedo-Suñer A CMOS preamplifier for electret microphones, *Proc. 1995 IEEE Int. Symp. Circuits Syst.*, **3**: 1995, pp. 1868–1871.
11. J. F. Duque-Carrillo *et al.* VERDI: An acoustically programmable and adjustable CMOS mixed-mode signal processor for hearing aid applications, *IEEE J. Solid-State Circuits*, **SC-31**: 634–645, 1996.
12. B. Stefanelli *et al.* A very low-noise CMOS preamplifier for capacitive sensors, *IEEE J. Solid-State Circuits*, **SC-28**: 971–978, 1993.
13. A. C. Pluygers A novel microphone preamplifier for use in hearing aids, *Analog Integr. Circuits Signal Process.*, **3**: 113–118, 1993.
14. L. Fasoli M. Sampietro Criteria for setting the width of *CCD* front end transistor to reach minimum pixel noise, *IEEE Trans. Elec. Dev.*, **ED-43**: 1073–1076, 1996.
15. J.-C. Bertails Low-frequency noise considerations for MOS amplifier design, *IEEE J. Solid-State Circuits*, **SC-14**: 773–776, 1979.
16. E. A. Vittoz The design of high-performance analog circuits on digital CMOS chips, *IEEE J. Solid-State Circuits*, **SC-20**: 657–665, 1985.

17. K. R. Laker W. Sansen *Design of Analog Integrated Circuits and Systems*, New York: McGraw-Hill, 1994.
18. E. Gatti P. F. Manfredi Processing the signals from solid-state detectors in elementary particle physics, *La Rivista del Nuovo Cimento*, **1**, serie 3, 1986.
19. V. Radeka Low-noise techniques in detectors, *Ann. Rev. Nucl. Part. Sci.*, **38**: 217–277, 1988.
20. A. Sartori *et al.* A 2-D photosensor array with integrated charge amplifier, *Sensors and Actuators A. Physical*, **46–47**: 247–250, 1995.
21. G. Bertuccio A. Pullia A low noise silicon detector preamplifier system for room temperature X-ray spectroscopy, *Proc. Symp. Semicon. Room-Temperature Radiation Detector Appl. Mater. Res. Soc. Symp. Proc.*, 302: 1993, pp. 597–603.
22. G. Bertuccio A. Pullia G. De Geronimo Criteria of choice of the front-end transistor for low-noise preamplification of detector signals at sub-microsecond shaping times for X- and γ-ray spectroscopy, *Nucl. Instr. Meth. Phys. Res.*, **A 380**: 301–307, 1996.
23. E. Gatti A. Hrisoho P. F. Manfredi Choice between *FETs* or bipolar transistors and optimization of their working points in low-noise preamplifiers for fast pulse processing: Theory and experimental results, *IEEE Trans. Nucl. Sci.*, **30**: 319–323, 1983.
24. G. Bertuccio L. Fasoli M. Sampietro Design criteria of low-power low-noise charge amplifiers in VLSI bipolar technology, *IEEE Trans. Nucl. Sci.*, **44**: 1708–1718, 1997.
25. I. Kipnis *et al.* A time-over-threshold machine: The readout integrated circuit for the BABAR silicon vertex tracker, *IEEE Trans. Nucl. Sci.*, **44**: 289–297, 1997.
26. J. Wulleman A low-power high-gain transresistance BiCMOS pulse amplifier for capacitive detector readout, *IEEE J. Solid-State Circuits*, **SC-32**: 1181–1191, 1997.
27. Z. Y. Chang W. Sansen Stability and noise performance of constant transimpedance amplifier with inductive source, *IEEE Trans. Circuits Syst.*, **CAS-35**: 264–271, 1989.

J. F. DUQUE-CARRILLO
University of Extremadura
GUIDO TORELLI
University of Pavia